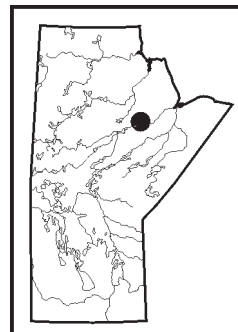


**New insights into the structural geology and timing of deformation at the Superior craton margin, Gull Rapids, Manitoba (NTS 54D6)**  
 by M.W. Downey<sup>1</sup>, S. Lin<sup>1</sup> and C.O. Böhm



Downey, M.W., Lin, S. and Böhm, C.O. 2004: New insights into the structural geology and timing of deformation at the Superior craton margin, Gull Rapids, Manitoba (NTS 54D6); *in* Report of Activities 2004, Manitoba Industry, Economic Development and Mines, Manitoba Geological Survey, p. 171–186.

### Summary

Structural mapping from the 2003 and 2004 field seasons has revealed at least five generations of ductile and brittle structures, termed  $G_1$  to  $G_5$ , with associated foliations, lineations, folds, and shears/faults. There are five main rock assemblages at Gull Rapids: basement granodiorite gneiss, possibly related to similar rocks in the adjacent Split Lake Block; mafic metavolcanic rocks (amphibolite); metasedimentary rocks; late-stage granitic and tonalitic intrusive rocks; and latest stage (Paleoproterozoic) mafic dikes. All rock types, except for the mafic dikes, are Archean and affected by the five generations of structures. The mafic dikes are only affected by the  $G_5$  event, which may be related to Hudsonian tectonothermal activity. Shear-zone kinematics during  $G_4$  reveal mostly south-side-up, dextral and sinistral movement along shear surfaces throughout the map area, and there is a reactivation of  $G_4$  shear zones by the  $G_5$  shearing event.

In addition, mapping has revealed three phases of felsic intrusion, in the form of sheet-like bodies and dikes. These dikes crosscut important structures, and are used to constrain the relative ages of structures in the map area. Radiometric dating is also being used to constrain the timing of deformation. Possible emplacement mechanisms for the voluminous felsic intrusions include passive emplacement along faults or in fold hinges, or more forceful emplacement via diking.

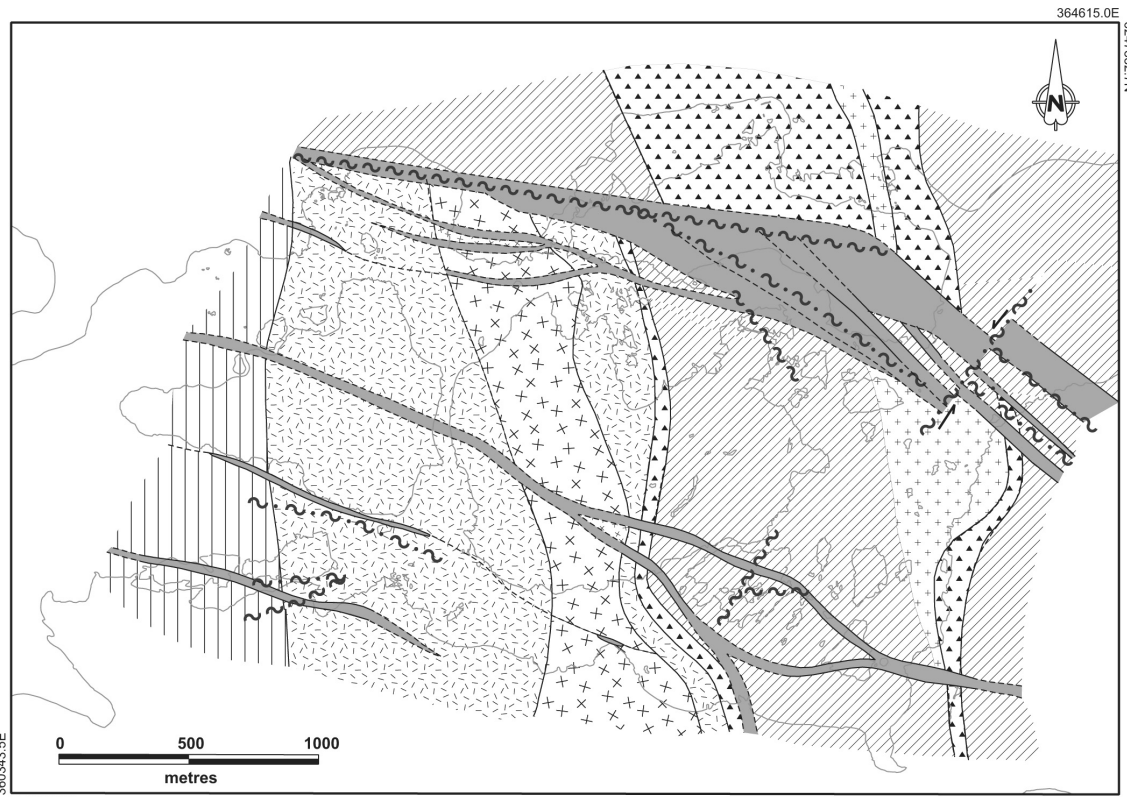
### Introduction

As part of the Manitoba Geological Survey's ongoing Superior craton margin program, structural mapping of the Gull Rapids area continued during the summer of 2004 (Böhm et al., 2003b). The Gull Rapids area is host to a spectacularly exposed sequence of multiply deformed Archean supracrustal and basement rocks that have been extensively studied over the past two years by researchers at the University of Waterloo, the Manitoba Geological Survey (Böhm et al., 2003a) and the University of Alberta (Bowerman et al., GS-14, this volume). The structural studies in 2004 included detailed 1:500- and 1:200-scale structural bedrock mapping, further collection of data on brittle and ductile structures, photographic analysis and further sampling, all to constrain the number and style of structural generations, the regional kinematics, the timing of deformation and the relationship between deformation and metamorphism in the area. A study of possible pluton-emplacement mechanisms and regional tectonics was also completed during the 2004 field season.

A detailed structural analysis (at micro-, meso- and macroscopic scales) of the supracrustal and basement rocks completed in 2003, along with the structural studies of 2004, combine to form the basis of research for the M.Sc. thesis of the senior author. The goal of this M.Sc. project is to obtain an understanding of the structure, kinematics and timing of deformation and metamorphism, to assist in the development of a model for the tectonic evolution of the Gull Rapids area, located at the Superior craton margin, a major collisional zone between the Archean Superior craton and the adjacent Proterozoic Trans-Hudson Orogen. The fieldwork is being complemented by microstructural thin-section studies at the University of Waterloo, and by the U-Pb dating of selected samples to obtain absolute ages of deformation.

Mapping and sampling at 1:5000, 1:1000, 1:500 and 1:200 scales in 2003 and 2004 identified two main crustal sequences: 1) an Archean amphibolite-facies supracrustal assemblage consisting of interbedded amphibolite (metabasalt) and iron-rich metagreywacke sequences, with interlayered banded iron formation, which is in structural contact with 2) Archean granulite-facies basement granodioritic and derived gneissic rocks of possible Split Lake Block age and origin (Figure GS-15-1; Böhm et al., 2003a). Multiple stages of leucocratic felsic injection invaded both supracrustal and basement rocks, and major east-southeast-trending Paleoproterozoic mafic dikes cut all of the above rock types (Figure GS-15-1). Using critical crosscutting relationships between structures in the supracrustal and basement rocks and the later felsic injection phases, the timing of deformation can be constrained by dating the intrusive phases. These issues, along with the suggested tectonic juxtaposition of the two crustal sequences, the structural relationship between the alternating sequences of metavolcanic and metasedimentary rocks, and the timing of felsic injection and dike emplacement, are discussed in this report.

<sup>1</sup> Department of Earth Sciences, University of Waterloo, Waterloo, Ontario N2L 3G1



### LEGEND

#### PALEOPROTEROZOIC

Mafic dykes (diabase and gabbro)

#### ARCHEAN FELSIC INTRUSIVE ROCKS

Granitoid injections and pegmatite subunits include leucogranite, granodiorite and tonalite

Granodiorite and derived gneiss

Granodiorite augen gneiss

Leucogranodiorite and derived gneiss

Granodiorite L-tectonite

#### ARCHEAN GULL RAPIDS SUPRACRUSTAL ROCKS

Metasedimentary rocks, metagreywacke, interlayered pelite and psammite

Mafic volcanic rocks, amphibolite interpreted as metabasalt, massive to laminated

Archean relative ages not implied

Geological contact (defined, inferred)

Ductile deformation zone (shear, fault)

Brittle deformation zone (intense jointing and fracturing)

**Figure GS-15-1:** Generalized geology of the Gull Rapids area (simplified after Böhm et al., 2003b).

## Structural geology

Structural investigations, using overprinting relationships and orientations and styles of structure, have revealed at least five generations of structures at Gull Rapids. The five generations of structures are hereby termed  $G_1$  to  $G_5$ , and the associated foliations, lineations and folds, where present, are termed  $S_1$  to  $S_5$ ,  $L_1$  to  $L_5$  and  $F_1$  to  $F_5$ , respectively. More than one generation of structure ( $G$ ) may appear within a single deformation event ( $D$ ), so the term ‘generation of structure’, rather than ‘deformation event’, is used to describe the structural geology of the multiply deformed Archean terrane at Gull Rapids. In the map area,  $G_1$  to  $G_3$  are represented entirely by ductile structures (foliations, lineations and folds), whereas  $G_4$  to  $G_5$  are represented by both ductile and brittle faulting. The timing of deformation is based on critical crosscutting relationships between the generations of structures and the felsic injection phases, and is being directly constrained by applying U-Pb dating to selected samples. Radiometric dating will help to determine if one specific generation of structure corresponds to one discrete deformation event.

## Foliation

The first foliation ( $S_1$ ) is a strong regional foliation that strikes approximately  $340\text{--}040^\circ$ , dips  $40\text{--}50^\circ\text{E}$ , and is roughly subparallel throughout the entire map area (Figure GS-15-2). Locally, the foliation dips subhorizontally, due to  $F_2$  folding (Figure GS-15-3). In metasedimentary rocks,  $S_1$  is a weak to strong schistosity that is represented by the alignment of mica grains and aggregates. In the metavolcanic rocks (amphibolite),  $S_1$  is a strong gneissosity that is represented by the compositional banding of more competent iron-, sulphide- and epidote-rich bands and less competent hornblende- and pyroxene-rich bands, where hornblende is elongated parallel to the foliation. In the granodiorite gneiss,  $S_1$  is a weak to strong gneissosity that is represented by the compositional banding of tonalite and granodiorite. Granodiorite gneiss can be structurally subdivided into three subparallel zones: 1) augen gneiss, 2) straight-layered gneiss, and 3) L>S- and L-tectonite gneiss (Figure GS-15-1). These zones trend subparallel to  $S_1$ , where  $S_1$  is defined by the alignment of flattened augen in augen gneiss, and by compositional banding (granodiorite to tonalite) in the straight-layered gneiss. The zone of augen gneiss may represent an approximately 400 m wide north-trending shear zone, but

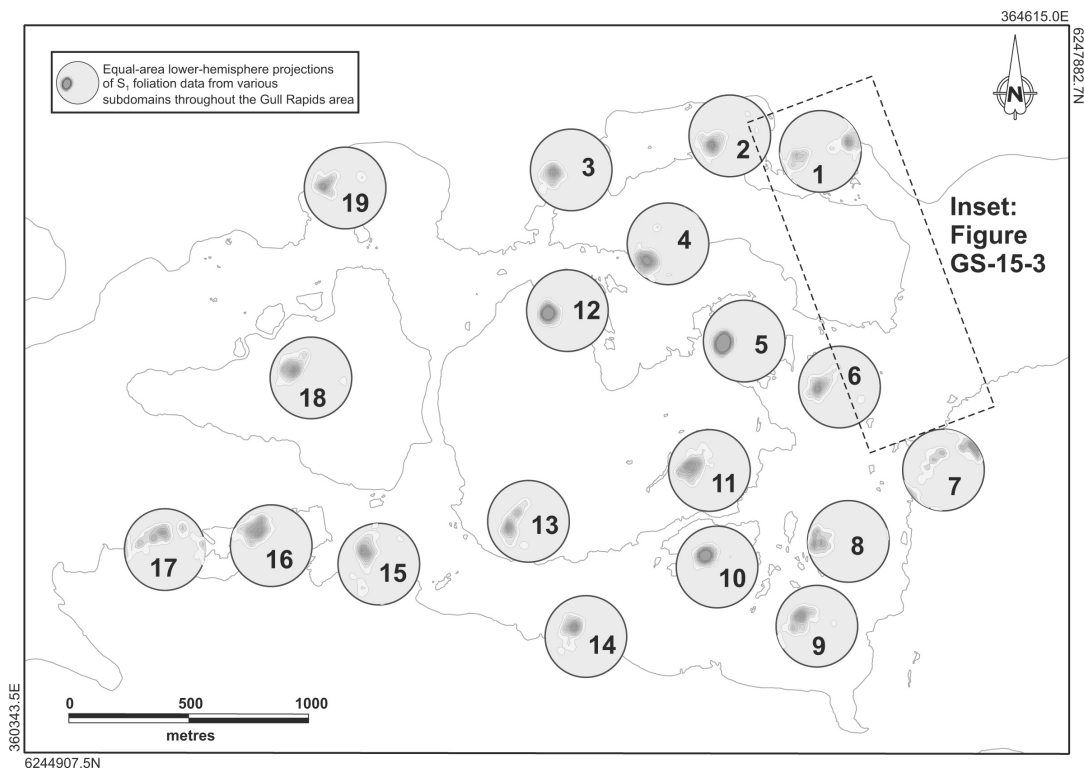


**Figure GS-15-2:** Equal-area lower-hemisphere stereoplots of  $S_1$  foliation measurements from 19 geological subdomains throughout the Gull Rapids map area (see Figure GS-15-1 for geology). Note general subparallelism of foliation, as well as some folding of the foliation by  $F_2$  (e.g., plots 1, 6, and 7 in the metasedimentary rocks, and plots 15 and 17 in the granodiorite gneiss). In the easternmost portion of the map area, possible major  $F_2$  axial planes can be traced from north to south along strike in the amphibolite (see Figure GS-15-3a).

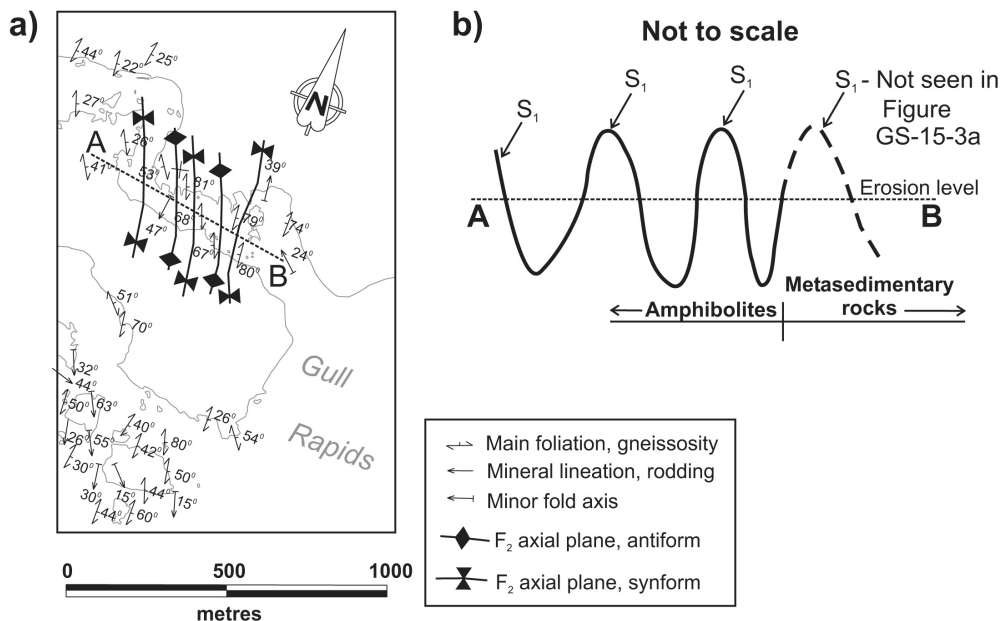


**Figure GS-15-3:** Structural measurements showing major  $F_2$  folding in the easternmost portion of the supracrustal rocks, Gull Rapids map area (see Figure GS-15-2 for location): **a)** several tight to isoclinal,  $F_2$  axial planes can be traced from north to south in the northern amphibolite (see Figure GS-15-1); here,  $S_1$  is steeply dipping to the west on the eastern flanks of the folded area, and is then folded over a number of times in a series of steep antiforms and synforms until, on the western flanks of the folded area,  $S_1$  returns to the regional dip direction of east; note that this folding is not seen in the metasedimentary rocks in the bottom half of the map area; **b)** schematic cross-section along AB in Figure GS-15-3a, showing folded sequence of  $S_1$  in the amphibolite; regional  $S_1$  is steepest here, and axial planes are parallel to  $S_1$  due to isoclinal folding.

augen are rarely asymmetric and give no clear sense of shear. Augen increase in number and are better preserved or developed toward the boundaries of the augen-gneiss zone. In addition, augen are flattened parallel to local  $S_1$  foliations and are stretched subparallel to regional stretching lineations.

Where bedding ( $S_0$ ) can be recognized in the metasedimentary rocks, it parallels  $S_1$ ; however, the distinction between  $S_0$  and  $S_1$  is typically difficult to make clearly in outcrop. The main  $S_1$  foliation is interpreted to be axial planar to  $F_1$ . In supracrustal sequences, this foliation is commonly deformed by  $F_2$  folds that only rarely have an axial-planar  $S_2$  foliation. This may mean that the temperature was not high enough to form an axial-planar foliation during the  $F_2$  folding event. Where seen,  $S_2$  is subparallel to  $S_1$ . A microstructural analysis of  $F_2$  fold hinges in selected metasedimentary samples is currently being completed in order to determine the crosscutting relationships between  $S_0$ ,  $S_1$  and  $S_2$ , and to analyze if a second foliation does indeed exist in many localities. This analysis will also help to determine which peak and retrograde metamorphic minerals define which foliation.

The  $S_1$  foliation appears to be transposed into  $S_2$  locally within the supracrustal rocks. This transposition is due to the tight to isoclinal  $F_2$  folding of  $S_1$ , with the  $S_2$  foliation being subparallel to  $S_1$ . The best evidence for transposition can be observed in layered amphibolite, where the gneissosity is strongest, and where there is a significant amount of tight to isoclinal folding of this strong  $S_1$  fabric. Because of the tight to isoclinal folding, however,  $F_2$  axial planes become parallel to  $S_1$ , and it is therefore difficult to distinguish a first foliation from a second transposition foliation. Therefore, it cannot be said for certain that there is an actual transposition of  $S_1$  to  $S_2$  everywhere in the supracrustal rocks.

The foliations described above are tectonic in origin. The late-stage granite injection phases, in sheet- and dike-like form, postdate  $S_1$  and seem to lack a foliation in most localities. The latest stage of granite injection, however, has been interpreted to be late syn- $G_1$  based on field observations, so these granitic sheets and dikes should have at least developed some  $S_1$  foliation. Indeed, a foliation within the granitic sheets and dikes can be locally observed, but the origin of this foliation is uncertain. This foliation seems to be parallel to sheet and/or dike boundaries, rather than being parallel to the local tectonic foliation in the surrounding host rocks. This leads to the question of whether or not the foliation within these granitic sheets and dikes is magmatic or tectonic in origin (Figure GS-15-4a, b).

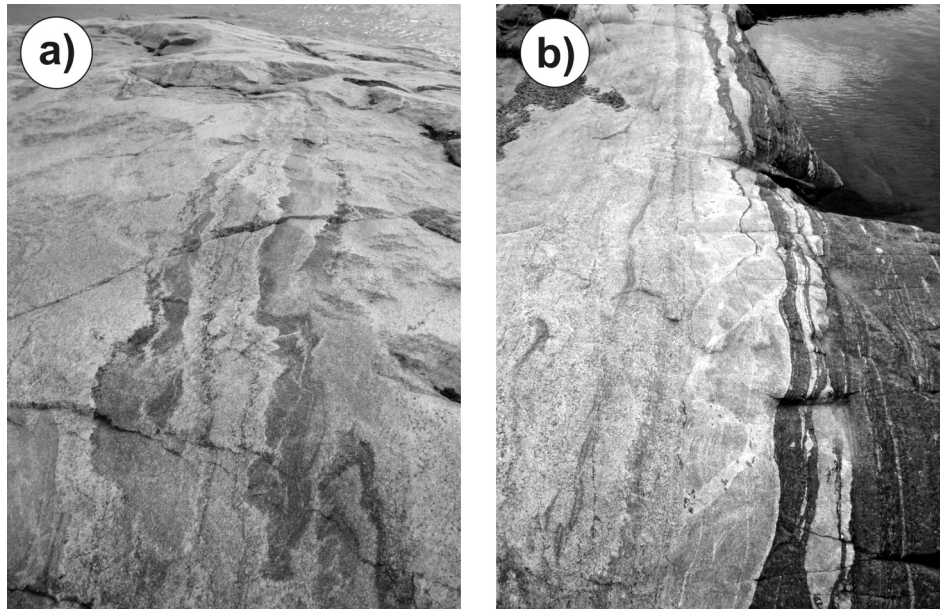


**Figure GS-15-4:** Outcrop photographs of magmatic and tectonic foliations, Gull Rapids map area: **a)** magmatic foliation in leucogranite dike; and **b)** magmatic foliation in white leucogranite dike (left side of photo), which is subparallel to the tectonic foliation ( $S_1$ ) in metasedimentary rocks (right side of photo). See text for discussion.

### **Lineations**

Only one generation of lineation,  $L_1$ , has been observed in rocks of the Gull Rapids area (Figure GS-15-5). This  $L_1$  lineation is most predominant in the metasedimentary rocks, and in portions of the granodiorite gneiss, where  $L_1$  lies on  $S_1$  foliation planes. It is a strong, moderately to shallowly plunging, stretching lineation that trends approximately south in the granodiorite gneiss and southeast in the metasedimentary rocks (Figure GS-15-5). In the metasedimentary rocks,  $L_1$  is defined by the preferred orientation of elongate biotite grains or aggregates (Figure GS-15-6a), whereas, in the granodiorite gneiss, it is defined by elongate quartz and feldspar (Figure GS-15-6b). Where seen,  $F_2$  minor fold axes are commonly parallel to  $L_1$  lineations (Figure GS-15-7).

The westernmost zone of granodiorite gneiss in the Gull Rapids map area is dominated by  $L>S$ - and  $L$ -tectonite (where the strain ellipsoid is of constrictional type, with  $K \gg 1$ ; Lin and Jiang, 2001). Moving across strike from east to west within the granodiorite gneiss, the structure changes from  $S$ - and  $S>L$ -tectonite to  $L$ - and  $L>S$ -tectonite (see Figure GS-15-1). This change occurs rather suddenly, and the transition zone between the dominantly  $S$ -tectonite and dominantly  $L$ -tectonite is approximately 30 m wide. Due to the small amount of available outcrop (only along the shores of the Nelson River), however, proper boundary conditions cannot be placed on the formation of this  $L$ -tectonite zone (cf. Knee Lake Shear Zone of Lin and Jiang, 2001). Regardless, the lineation in the  $L$ -tectonite trends subparallel to lineation throughout the map area, suggesting that all lineations at Gull Rapids are kinematically related.

### **Boudinage**

Boudinage is limited to the supracrustal rocks, and is related to the  $S_1$  foliation. Boudinage is best seen in the layered amphibolite, where the competency contrast between compositional layers is highest. Competent iron-, sulphide-, and epidote-rich calcsilicate layers contrast against less competent hornblende- and pyroxene-rich layers (Figure GS-15-8a, b). In most cases within the layered amphibolite, the competency contrast is such that moderate pinch-and-swell structures are observed (Figure GS-15-8a). Locally, the boudins are less necked because the competency contrast is higher. This leads to the formation of rectangular-style boudins (Figure GS-15-8b). In the metasedimentary rocks, iron formations, subparallel to bedding and  $S_1$ , are much more competent than the predominant metagreywacke and metapelite layers. This competency contrast leads to pervasive boudinage of the iron formation and, to a lesser extent, of the host metasedimentary rocks (Figure GS-15-8c).

Boudinage throughout the Gull Rapids area is interpreted as being late syn- $G_1$  to early-syn- $G_2$  because boudinage affects  $S_1$  foliations, yet is folded by  $F_2$  (Figure GS-15-8d). In a few localities within the amphibolite, there is pegmatitic

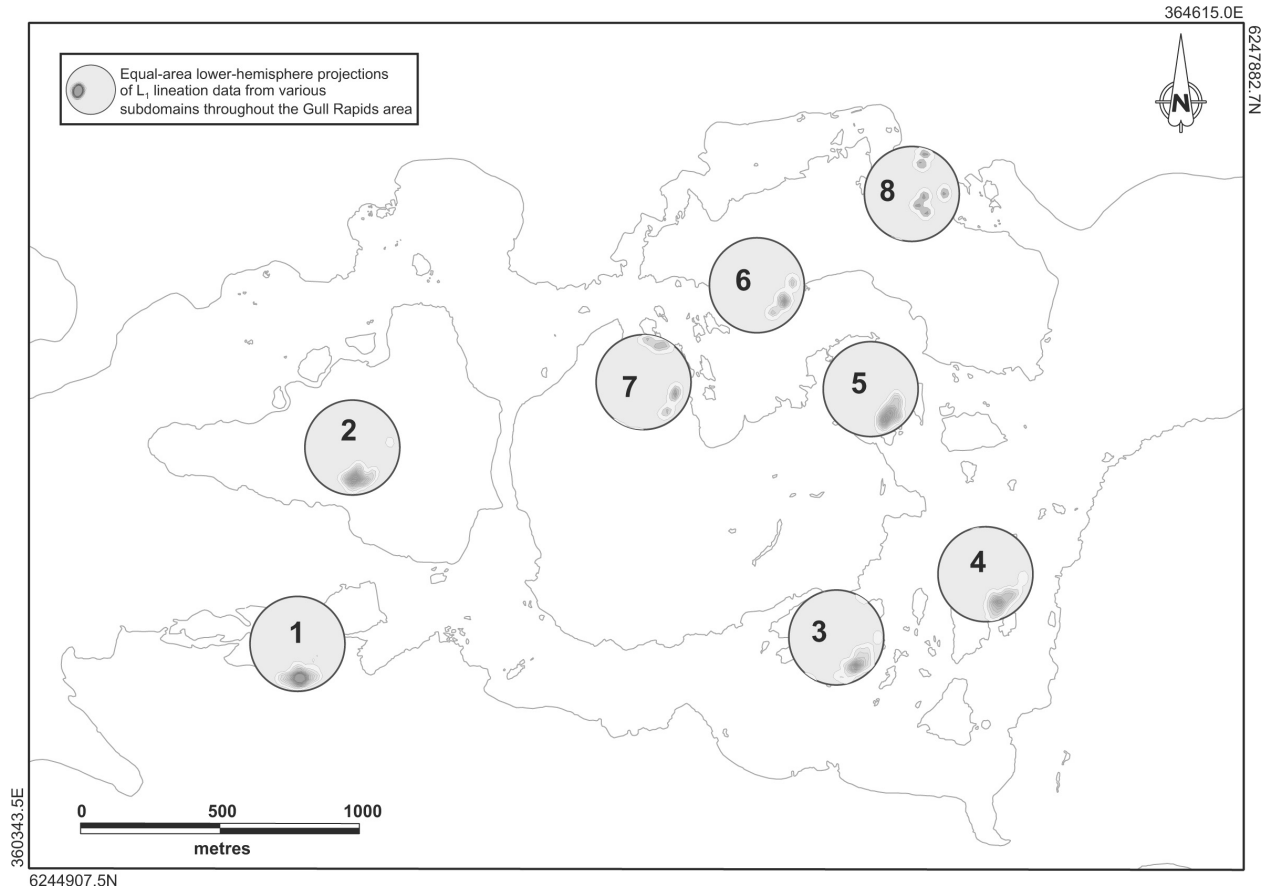


**Figure GS-15-5:** Equal-area lower-hemisphere stereoplots of  $L_1$  lineation measurements from eight geological subdomains throughout the Gull Rapids map area (see Figure GS-15-1 for geology). Note the general subparallelism of lineation throughout the map area; however, in the granodiorite gneiss (plots 1 and 2), the lineations plunge moderately shallowly to the south, whereas, in the metasedimentary rocks (plots 3, 4, 5 and 6), they plunge moderately shallowly to the southeast. Plots 7 and 8 (in the augen gneiss and layered amphibolite, respectively) show some doubly plunging lineations.

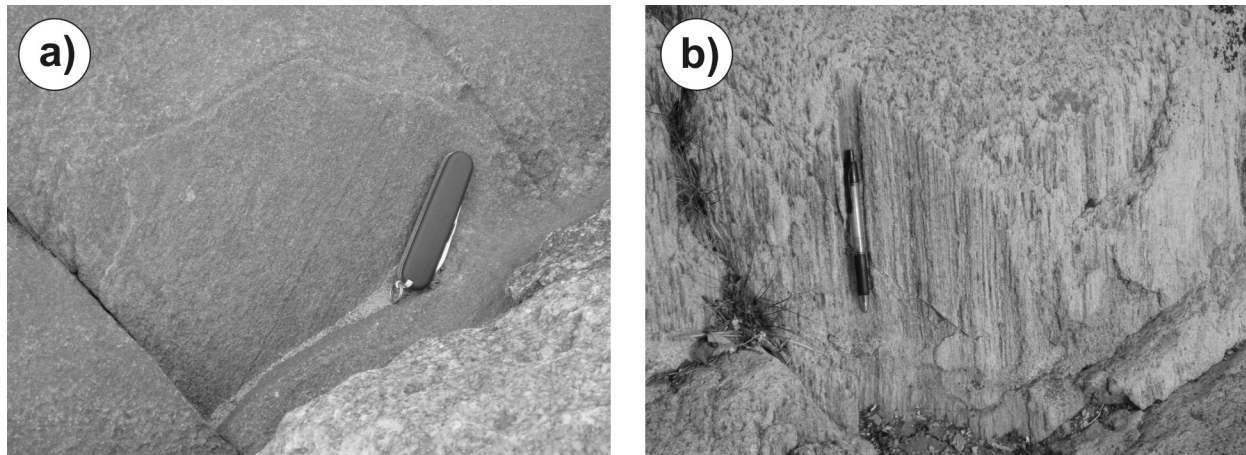
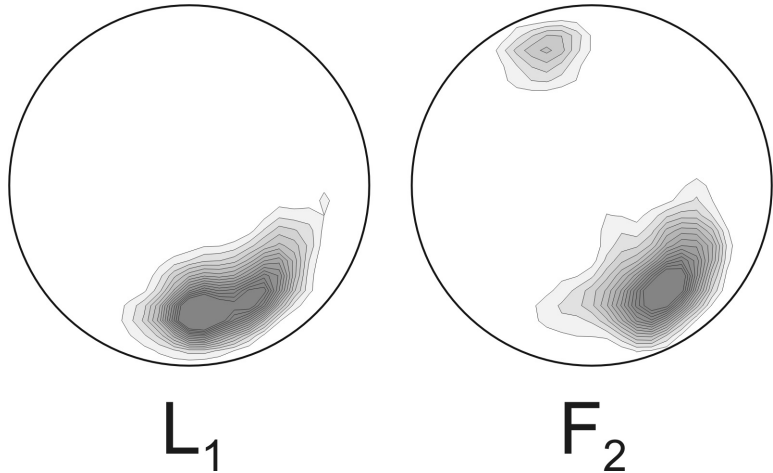


**Figure GS-15-6:** Outcrop photographs of lineations, Gull Rapids map area: **a)** stretched biotite representing strong  $L_1$  stretching lineation in metasedimentary rocks;  $L_1$  lies on  $S_1$  surface (knife is parallel to lineation); **b)** stretched quartz and feldspar in L-tectonite granodiorite gneiss (pen is parallel to lineation); strong stretching direction is subparallel to regional  $L_1$ .

**Figure GS-15-7:** Equal-area lower-hemisphere stereoplots of  $L_1$  lineation measurements and  $F_2$  minor fold axis measurements from throughout the Gull Rapids map area. Note that  $L_1$  and  $F_2$  are subparallel, which could indicate that  $L_1$  and  $F_2$  formed at different times during a single deformation event under one particular field of stress, or that  $L_1$  formed during one deformation event, under one particular field of stress, and was followed by  $F_2$  forming during a second deformation event under a different, yet parallel, field of stress. Note also that  $F_2$  is doubly plunging (see below).



granite injection into boudin necks. This injection is interpreted to be syn-boudinage (Figure GS-15-8e). Since the boudinage has been interpreted to be late syn- $G_1$  to early syn- $G_2$ , geochronological samples of the syn-boudinage pegmatitic granite injection were taken to constrain the absolute age of the later stages of  $G_1$  and/or the earlier stages of  $G_2$ .

### Folding

Within the map area, there are a number of generations of folding,  $F_1$  to  $F_3$ , with the most predominant generation being  $F_2$  (Figure GS-15-9). With the exception of local shear-related folding in the granodiorite gneiss, folding is only observed within the supracrustal rocks. The  $F_1$  generation is an upright, isoclinal style of folding, with an axial surface striking approximately north-south. It is best developed in the metasedimentary rocks where bedding is seen to be isoclinally folded by  $F_1$ . It also folds the original unconformities between the metasedimentary rocks and the amphibolite (repetition of supracrustal units in Figures GS-15-1 and -3). The  $S_1$  foliation is widespread and interpreted to be an  $F_1$  axial-planar foliation because, in metasedimentary rocks, it is always parallel to observed  $F_1$  axial surfaces and, in the amphibolite, it is usually steeply dipping, similar to the orientation of contained upright  $F_1$  folds.

The second generation of folding,  $F_2$ , is a moderately plunging, tight to isoclinal style that always folds  $S_1$ . It plunges southeast throughout most of the map area, except in amphibolite in the northeastern portion, where it plunges northwest (Figures GS-15-7 and -9). This transition from a southeast plunge to a northwest plunge is most likely due to deformation during third-generation folding ( $F_3$ ). Large-scale  $F_2$  folding of  $S_1$  can be observed in some localities within the supracrustal rocks (Figure GS-15-3); however, minor M-, S- and Z-shaped, tight to isoclinal  $F_2$  folds are common throughout the supracrustal rocks (Figure GS-15-10a, b). Locally, these minor folds are more open (see Böhm et al., 2003a, Figure GS-13-7). The stereographic plot shows that the minor  $F_2$  folding of  $S_1$  is of the same generation as the major  $F_2$  folding in the supracrustal rocks (Figure GS-15-11). These minor folds are therefore parasitic to the major folds (Figures GS-15-3 and -11).

The third generation of folding,  $F_3$ , is an open, generally upright style with an axial plane oriented approximately  $080^\circ/50^\circ\text{S}$ . The  $F_3$  generation rotates  $S_1$  (and  $S_2$ ) strike orientations from  $345\text{--}000^\circ$  in the northern portion of the supracrustal sequence to  $030\text{--}050^\circ$  in the southern portion (Figure GS-15-12a). This major fold has an amplitude of approximately 1 km. The  $F_3$  generation also refolds minor  $F_2$  axial planes and fold axes (Figures GS-15-10c, d, e, f, -12b). This small-scale refolding is only seen in a few localities within the supracrustal rocks, and is parasitic to the much larger  $F_3$  fold.

### Shearing and faulting

Shearing is late and comprises the structural generations  $G_4$  and  $G_5$ . In the supracrustal rocks, shearing is largely semibrittle and cuts all foliations, lineations and folds, and all rock types except the mafic dikes. In the granodiorite gneiss, ductile shearing, typical of Archean gneissic bodies, is observed. It is also relatively late, as it cuts the gneissosity. Shearing, of unknown age, may be responsible for the juxtaposition of the basement gneiss and overlying supracrustal rocks; however, this juxtaposition may just be an unconformity. The difference between the supracrustal rocks being semibrittle and the gneiss being ductile may be due to a compositional or rheological contrast between the supracrustal

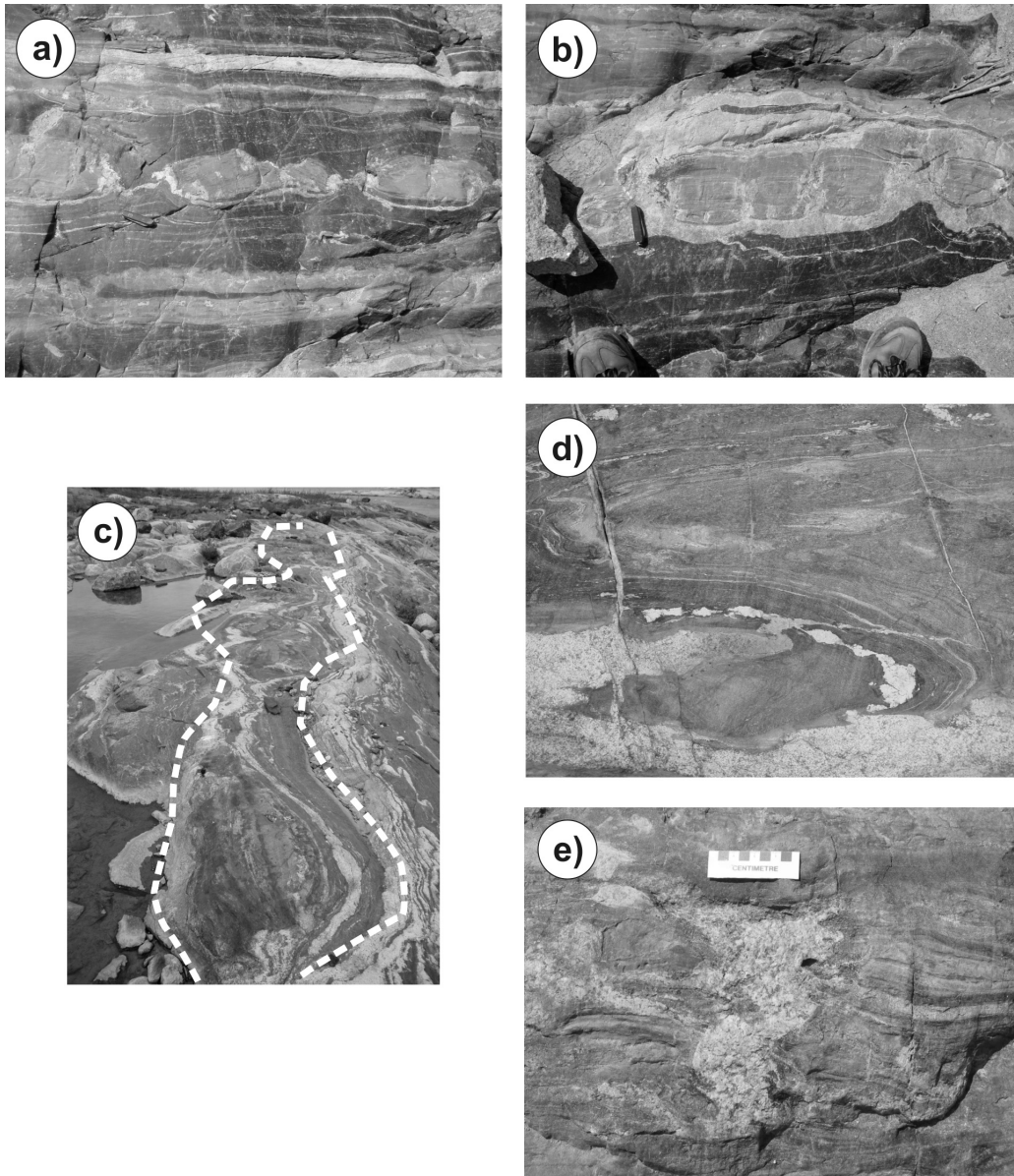


**Figure GS-15-8:** Outcrop photographs of boudinage, Gull Rapids map area: **a)** competency contrast, in layered amphibolite, between competent iron-, sulphide-, and epidote-rich calcisilicate layers and less competent hornblende- and pyroxene-rich layers; note the moderate pinch-and-swell structures, where there is a lenticular shape to the necked boudins; **b)** rectangular-style boudinage in layered amphibolite; note the lack of boudin necks and the fact that the boudins have a rectangular cross-section rather than a more lenticular one; **c)** boudinage of iron formation in metasedimentary rocks (iron formation outlined); **d)** late syn- $G_1$  to early syn- $G_2$  boudinage that has been folded by  $F_2$ ; note that the boudinaged layer is a white granitic dikelet that initially cuts  $S_1$ , but then was boudinaged and folded around a moderately tight  $F_2$  fold; **e)** syn-boudinage granitic dikelet, with dike material injected into boudin necks, which are interpreted to be late syn- $G_1$ .

rocks and the orthogneiss, and is probably not related to depth, because both the orthogneiss and the supracrustal rocks were at the same crustal level during the late shearing, as there is no deformation (i.e., folding) after shearing.

At mafic dike contacts within the metasedimentary rocks, shearing is entirely brittle, as evidenced by the presence of pseudotachylite veining and fault gouge, subparallel to some contacts (Figure GS-15-13a, b). Mafic dike contacts are zones of weakness that facilitate the concentration of late brittle shearing at or near those contacts (Figure GS-15-13c). Some shears cut and shear the mafic dikes, whereas others are themselves cut by the dikes (Figure GS-15-13d).

The  $G_4$  shearing strikes east-northeast, is more ductile than brittle (yet still semibrittle), has components of dip and strike slip (oblique slip), and is always south-southwest side up, while being both dextral and sinistral (Figure

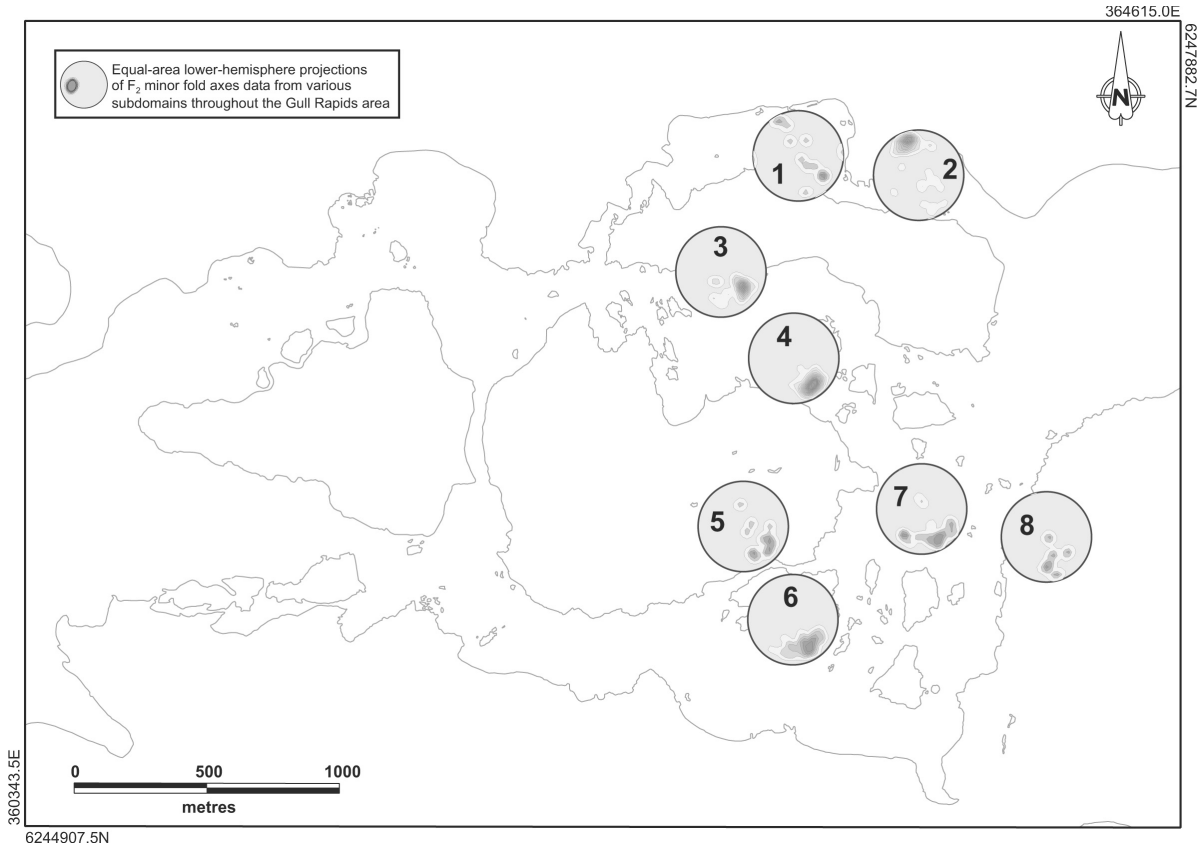


**Figure GS-15-9:** Equal-area lower-hemisphere stereoplots projections of  $F_2$  minor fold axis measurements from eight geological subdomains in the eastern part of the Gull Rapids map area. Folding in the granodiorite gneiss (western part of map area) has not been observed. Plots 1, 5 and 8 are poorly constrained because of a lack of measurable fold axes; however, plots 2, 3, 4, 6 and 7 are much better constrained and show that the  $F_2$  minor fold axes generally are south-east-trending, moderately plunging, open to tight folds. The  $F_2$  minor fold axes are parallel to  $L_1$  stretching lineations. The best constrained plots, 2, 4 and 6, clearly show that  $F_2$  plunges southeast in the metasedimentary rocks (plots 4 and 6) but plunges northwest in the amphibolite (plot 2). This may be due to upright open  $F_3$  folding, with an axial plane striking approximately east. See text for further discussion.

GS-15-14). The  $G_4$  shearing seems to have occurred at a medium to high metamorphic grade (amphibolite), based on the metamorphic mineral assemblage, and always predates mafic dike emplacement, as mafic dikes cut across  $G_4$  shears. The  $G_5$  shearing also strikes east-northeast and is more brittle than ductile (yet still semibrittle), dominantly strike slip and both dextral and sinistral (Figure GS-15-14). The  $G_5$  shearing seems to have occurred at a medium to low metamorphic grade (greenschist) and always postdates mafic dike emplacement, as mafic dikes are cut by  $G_5$  shears, although this shearing is preferential at mafic dike contacts. The  $G_5$  shearing may be related to Hudsonian deformation, as  $G_5$  shears cuts mafic dikes that have been dated at 2073 Ma (Heaman and Corkery, 1996).

In a few localities,  $G_4$  faults are reactivated during  $G_5$ . In one example, the earlier shearing ( $G_4$ ) is dextral and southwest side up, as evidenced by oblique slickenlines on the shear surface, and the later shearing ( $G_5$ ) is sinistral, as evidenced by horizontal ridge-and-groove-type slickenlines. The earlier shearing contains metamorphic minerals in the slickenlines indicative of high, prograde metamorphism (hornblende, pyroxene), whereas the later shearing contains metamorphic minerals in the slickenlines indicative of later greenschist-facies retrograde metamorphism (chlorite). Greenschist-facies retrograde metamorphism usually occurs first in shear zones, probably because they are conduits for fluids, whereas the host amphibolite- and granulite-grade rocks are tighter and reach greenschist-grade metamorphism later during their retrogression. In another example, the earlier shearing ( $G_4$ ) is more ductile than brittle, and has a dextral, southeast-side-up shear sense, as evidenced by S-C fabrics. The later shearing ( $G_5$ ), further along strike, is more brittle and sinistral, as evidenced by S-C fabrics and a sheared mafic dike with fault gouge at its hostrock contact. Therefore,  $G_4$  shearing is generally interpreted to be oblique and largely dextral, predating mafic dike emplacement, whereas  $G_5$  shearing displays only a strike-slip component, is largely sinistral and postdates mafic dike

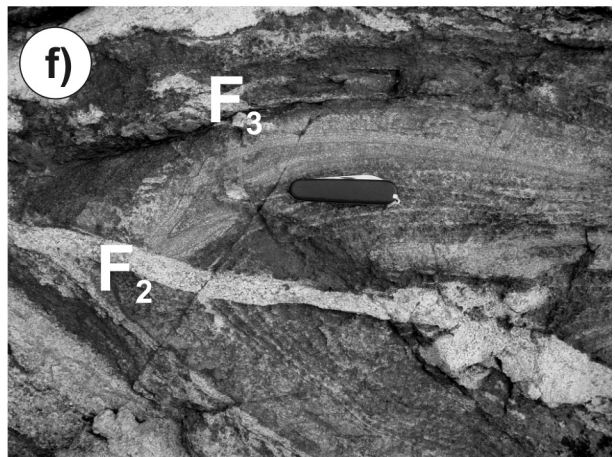
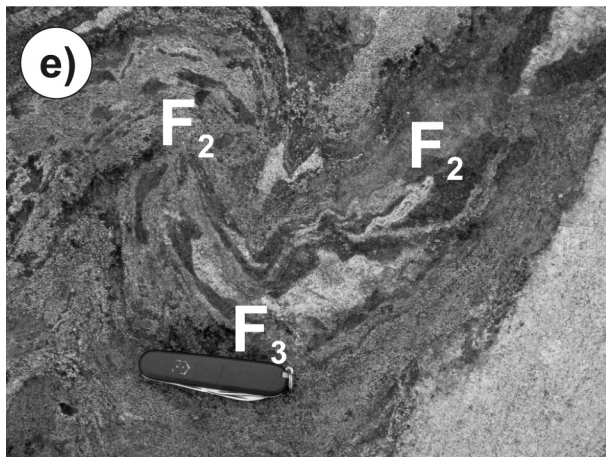
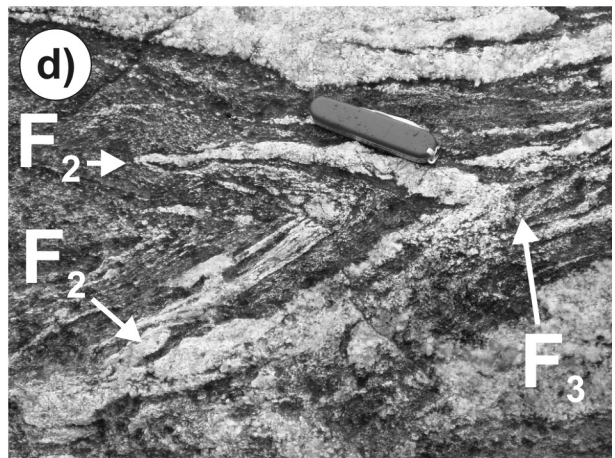
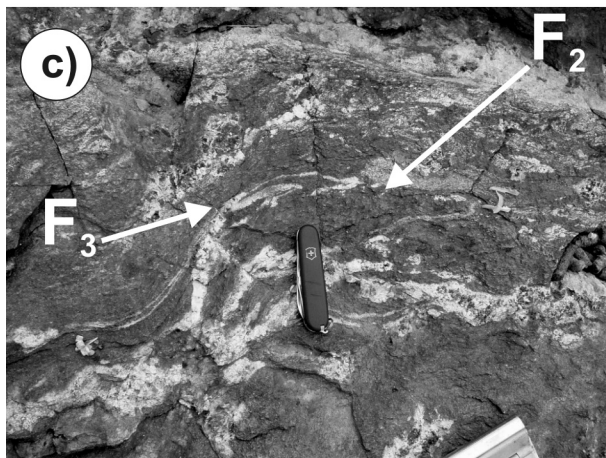
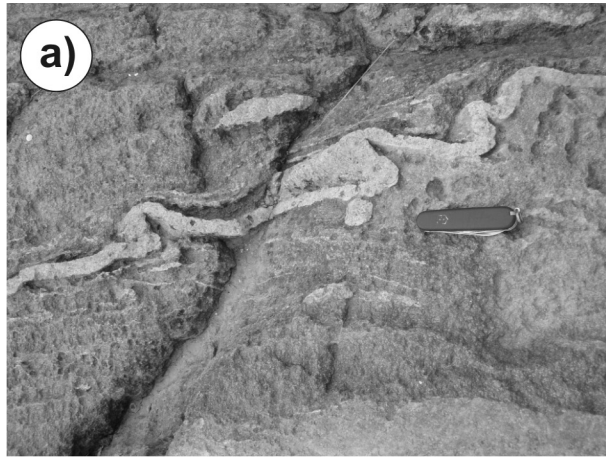


**Figure GS-15-10:** Outcrop photographs of folding, Gull Rapids map area: **a)** typical S-fold of  $S_1$ -parallel granitic injection dikelet in metasedimentary rocks; **b)** nicely exposed tight to isoclinal upright  $F_2$  fold in the layered amphibolite; **c), d), e)** and **f)** examples of refolded folds in metasedimentary rocks, in which  $F_2$  is refolded by  $F_3$  and  $F_2$  axial surfaces are always tight to isoclinal and being refolded by more open-style  $F_3$  axial surfaces.

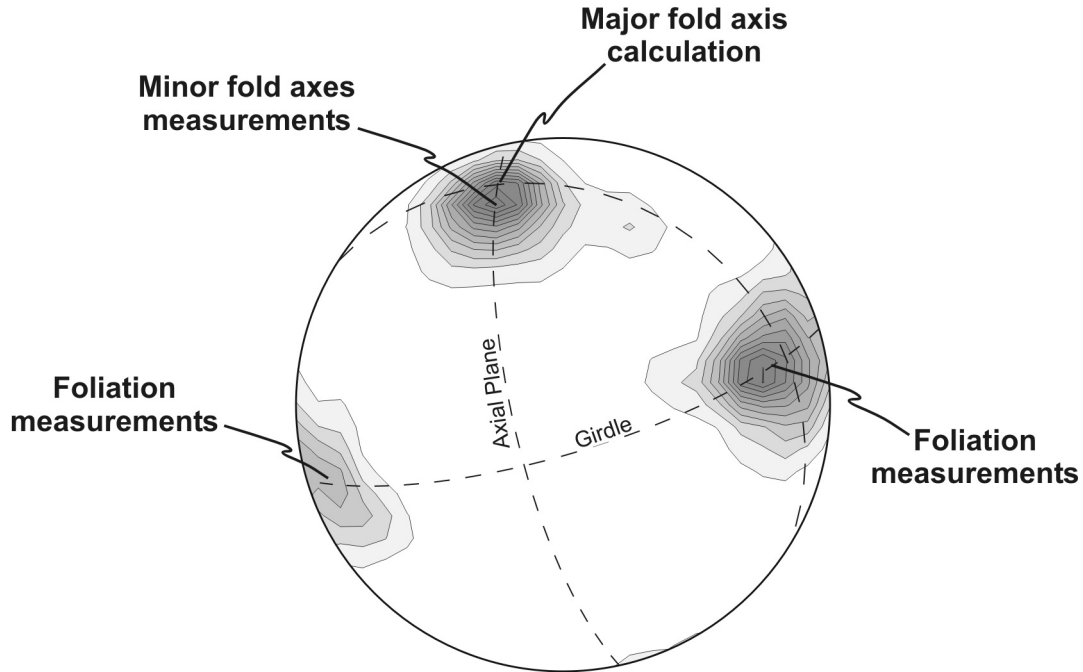


**Figure GS-15-11:** Equal-area lower-hemisphere stereoplots projection of  $F_2$  minor fold axis and  $S_1$  foliation measurements from a single geological subdomain within amphibolite. Foliations were measured and plotted, and the style (tight to isoclinal), axial plane (strike and dip of approximately  $170^\circ/80^\circ W$ ) and fold axis (pole to girdle, trend and plunge of approximately  $350^\circ/20^\circ$ ) of the major  $F_2$  folds were calculated. Minor fold axes are plotted on the same stereoplots, and the measured minor  $F_2$  fold axes were found to be parallel to the calculated major  $F_2$  fold axis, indicating that both of these styles of folding within the supracrustal rocks belong to  $F_2$ . Note also that the fold axis is plunging toward the northwest; this plunge direction is unique to this subdomain and may be a result of  $F_3$  folding (the normal plunge direction of  $F_2$  folds in the supracrustal rocks is to the southeast).

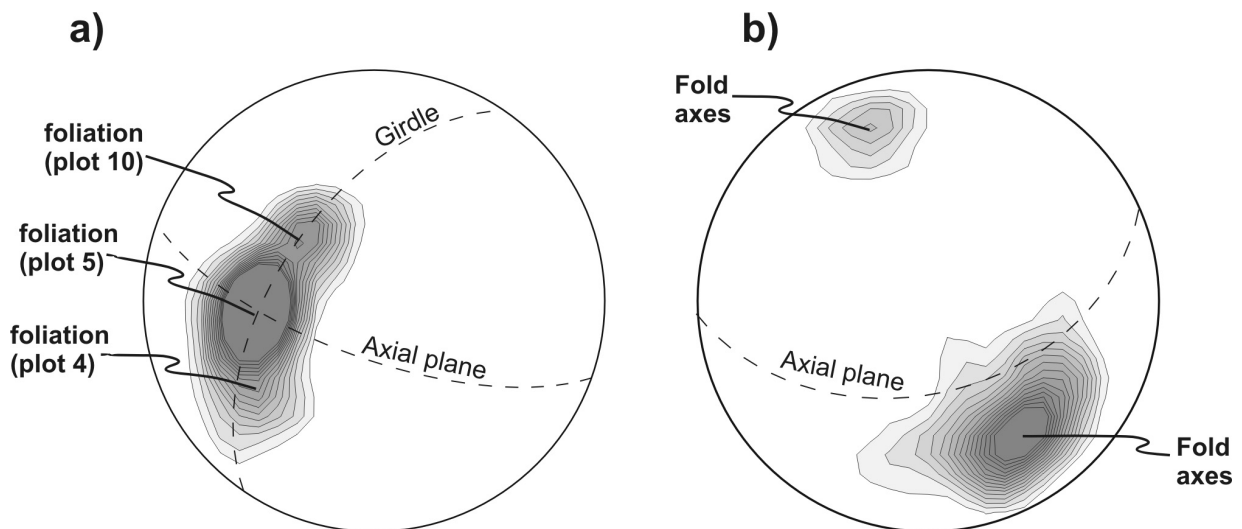


**Figure GS-15-12:** Equal-area lower-hemisphere stereoplots projections of possible  $F_3$  folding using  $S_1$  foliation measurements and  $F_2$  minor fold axes from three subdomains in the supracrustal rocks, Gull Rapids map area: **a)** foliation measurements (from plots 4, 5, and 10 on Figure GS-15-2) are folded in an open to tight style; minor  $F_2$  fold axes are refolded in these subdomains; **b)** minor fold axes plunge to the northwest and southeast, indicating refolding of  $F_2$ ; fold axes lie on folded  $S_1$  surfaces. From (a) and (b),  $F_3$  is an open, upright fold generation with an axial plane striking approximately  $080^\circ$  and dipping approximately  $40\text{--}50^\circ S$  (axial plane as seen in b).

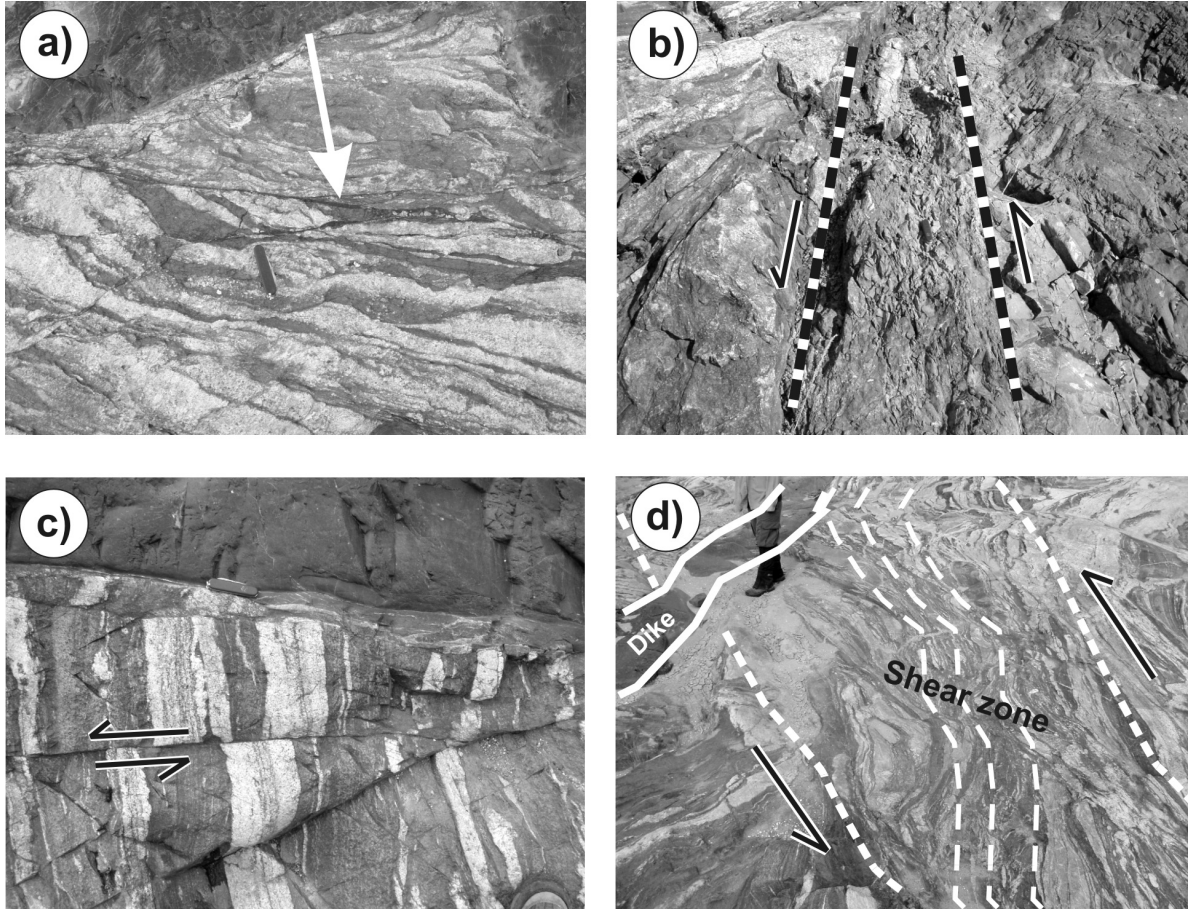


**Figure GS-15-13:** Outcrop photographs of shearing and faulting, Gull Rapids map area: **a)** pseudotachylite veining in a brittle shear zone (arrow points to black vein); **b)** fault gouge in a semibrittle sinistral shear zone at a mafic dike contact (the fault gouge zone, shown between dashed lines, is a 30 cm wide shear zone between metasedimentary rocks to the left and the mafic dike to the right); **c)** brittle sinistral fault cuts metasedimentary rocks and injection, near mafic dike contact (mafic dike is at top of photo); **d)** semibrittle sinistral shear zone in metasedimentary rocks cut by mafic dike (shearing is therefore  $G_4$ ); solid lines outline the mafic dike, thick dashed lines outline the shear zone, and thin dashed lines represent sinistral shear bands within the shear zone.

emplacement (Figures GS-15-13, -14).

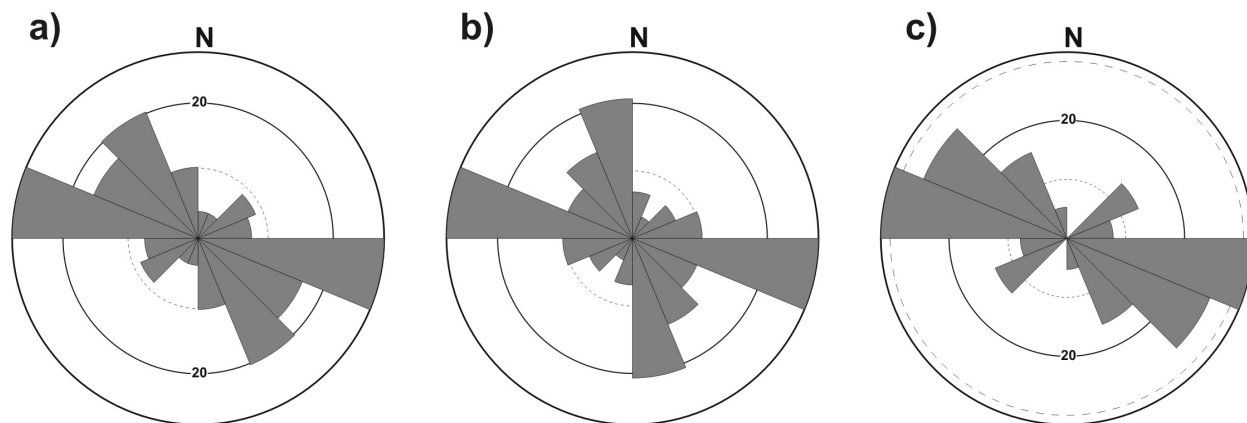
In one subdomain within the metasedimentary rocks, a sinistral, extensional-type fault is accompanied by pegmatite dike emplacement, which is most likely related to  $G_4$  shearing because a mafic dike cuts this shear zone. A dip-slip component of this faulting is not evident. This extensional fault is also parallel to the main easterly direction of faulting. Bookshelf-style faulting accompanies this extensional shearing and results in an overall sinistral sense for the shear zone (Figure GS-15-15).

### Jointing

Joint-set data were collected during the summers of 2003 and 2004 for the geological engineering study being completed at Manitoba Hydro's proposed Gull Rapids hydroelectric dam site. The majority of joint sets strike east (Figure GS-15-16). Joints and related late-stage fractures affect all rock types and structures. Joint sets were not grouped into a structural generation because they are always the youngest; however, some older joints can be grouped into  $G_4$  and/or  $G_5$ .

### Timing of deformation

The relative timing of deformation at Gull Rapids is constrained by using crosscutting relationships between structures and felsic intrusive phases. Radiometric dating, using the U-Pb technique, is currently underway on selected



**Interval = 22.5**

**Figure GS-15-14:** Rose diagrams of strike orientations of shears and faults, Gull Rapids map area: **a)** all shear and fault measurements within the map area; note the two main orientations, a dominant easterly one and a subdominant south-easterly one; **b)** dextral shears and faults strike dominantly east and subdominantly south-southeast; **c)** sinistral shears and faults strike dominantly east and subdominantly east-southeast. Based on field observations,  $G_4$  shearing seems to be more dextral (east and south-southeast), whereas  $G_5$  shearing seems to be more sinistral (east and east-southeast).

samples of crosscutting felsic intrusive rocks to obtain absolute ages for a number of the structural generations.

Based on field observations, at least three main intrusive phases can be distinguished within the map area. In places, it is unclear whether these intrusive phases represent melt (leucosome) or injection, or a mixture of both. The first phase is granitic and is interpreted to have been emplaced late syn- $G_1$  to early syn- $G_2$ . Crosscutting relationships of this phase are best seen in the northern amphibolite, where this phase cuts  $S_1$ , is folded by  $F_2$  and is locally either boudinaged or syn-boudinaged (Figure GS-15-8d and e, respectively). Therefore, this early phase has to be post- $S_1$ , pre- $F_2$  and at least syn-boudinaged (late syn- $G_1$  to early syn- $G_2$ ). A sample of a syn-boudinaged dike is currently being dated by the U-Pb technique to constrain the absolute age of  $G_1$ . The presence of orthopyroxene in this early intrusive phase implies that it reached granulite metamorphic grade. Since no  $F_2$  axial-planar cleavages ( $S_2$ ) are developed in the amphibolite, the temperatures during  $G_2$  were probably not very high. All of the above evidence implies that the early, orthopyroxene-bearing intrusive phases are related to  $G_1$ , and were emplaced during  $G_1$  and prior to  $G_2$ . This is consistent with the correlation of metamorphism with deformation: peak metamorphism,  $M_1$ , correlates with the onset of deformation,  $G_1$ , in the area.

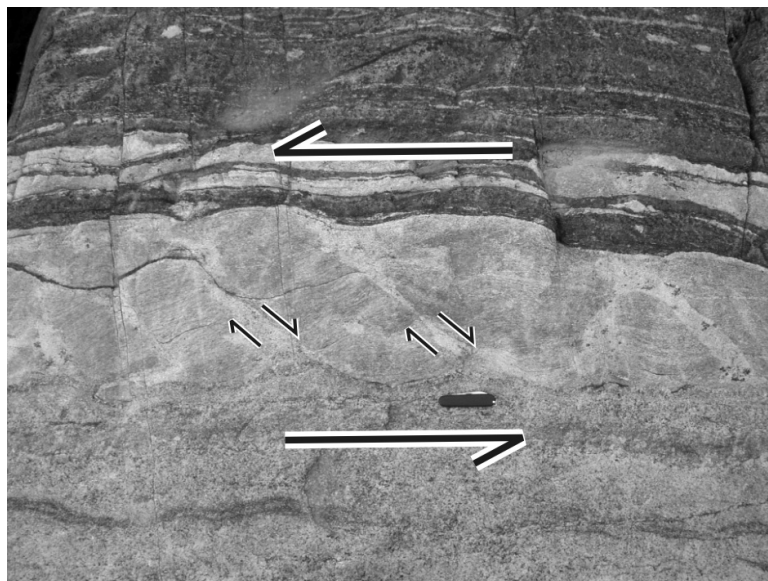


**Figure GS-15-15:** Outcrop photograph of sinistral bookshelf-style shearing, Gull Rapids map area. Small arrows indicate normal faulting of 'books', which gives an overall sinistral sense for the shear zone (large arrows). See text for discussion.

The early intrusive phase is widespread, and has a fairly prolonged period of emplacement. It comprises large, sheet-like granitic bodies, as well as smaller granitic dikes and dikelets. The larger granitic sheets cover much of the Gull Rapids area (Figure GS-15-17a) and appear to be late syn- $G_1$  to early syn- $G_2$  as well, because they crosscut  $S_1$  yet are

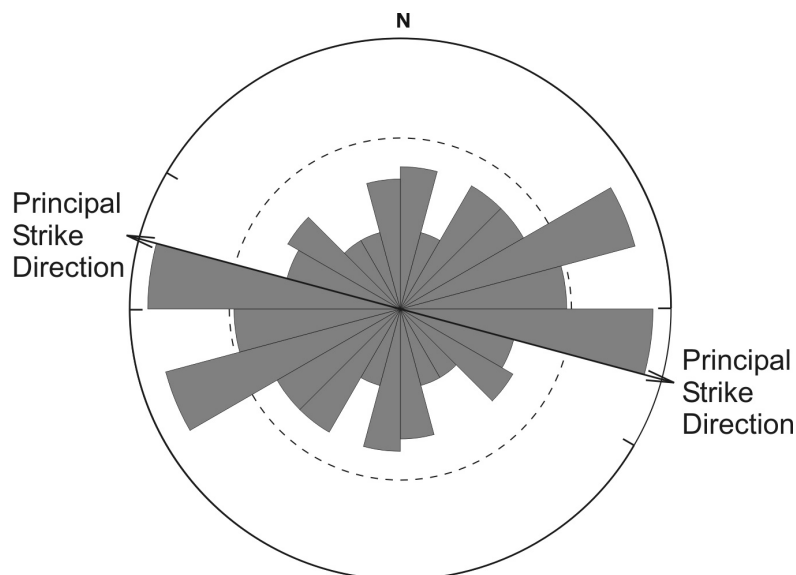


**Figure GS-15-16:** Rose diagram of strike orientations of joint measurements, Gull Rapids map area. There are a number of orientations of joint sets, but the majority strike approximately east.

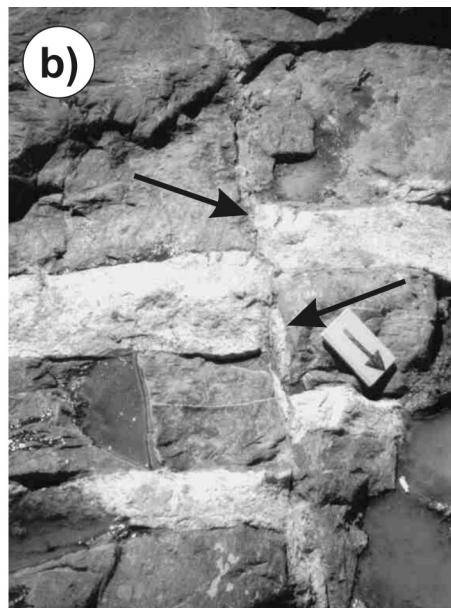


**Figure GS-15-17:** Outcrop photographs of intrusive phases, Gull Rapids map area: **a)** late syn- $G_1$  granitic sheet, covering metasedimentary rocks and  $S_1$ , yet also folded by  $F_2$  (arrow points to granitic sheet); **b)** pegmatite dike cut by shear zone with syn-shear injection along the fault plane (arrows point to shear zone and syn-shear pegmatite dike).

folded by  $F_2$ ; the folding is evidenced by dikes and dikelets that originate from these granitic sheets.

Most localities display only first and second intrusive phases. The second phase, also widespread, is composed of pegmatitic granite, and it occurs as straight-walled dikes and dikelets that cut all foliations, lineations, folds and rock types, except mafic dikes. This phase is always sheared, and is therefore pre- $G_4$ .

In a few localities, three intrusive phases show crosscutting relationships and likely predate  $G_4$ - $G_5$  where sheared, whereas some pegmatite of the second or third phase may be syn- $G_4$ - $G_5$  shearing. The latter was observed in one location, where a pegmatite dike crosscuts  $S_1$  at a low angle and becomes displaced by an east-striking, almost vertical shear zone, suggesting that emplacement predated shearing (Figure GS-15-17b). Unsheared, undisplaced pegmatite,

of similar appearance and composition to the displaced pegmatite dike, then fills in along the fault plane, suggesting that emplacement was also syn-shearing. Therefore, on the whole, this second phase of intrusion can be considered syn- $G_4$ - $G_5$  shearing. A sample of the syn-shearing pegmatite is currently being dated by the U-Pb technique to constrain the minimum age of  $S_1$ , as well as the age of  $G_4$ - $G_5$  shearing. In another location, a pegmatite dike appears to be controlled by a shear zone, as an approximately 30 cm wide shear zone runs straight through the middle of the 1 m wide, straight-walled pegmatite dike along its entire length.

The felsic intrusive phases at Gull Rapids (not including the granodiorite gneiss of the Split Lake Block) form a large volume of felsic magmatism. The cause of this magmatism, as well as mechanisms of intrusion emplacement, are an additional focus of this study. The emplacement of the Gull Rapids granitic sheets and dikes requires that space be made for that intrusive material in the crust. One possible mechanism is passive emplacement along faults or in fold hinges (there is significant faulting and folding at Gull Rapids). Another possible mechanism is forceful emplacement (e.g., a dike forces the wall rocks aside as it intrudes). Emplacement of the granite dikes locally affects structure in a forceful way in the northern amphibolite (Figure GS-15-18). These dikes and dikelets push aside the foliation and force their way into the zones of weakness between foliation planes.

### Economic considerations

This study is providing accurate and detailed bedrock maps and structural data of the Gull Rapids area for Manitoba Hydro and other land-use clients. The structural study of this area is of importance to both Manitoba Hydro, for geo-engineering purposes (e.g., detailed fracture analysis required for the construction of a hydroelectric dam), and to mineral-exploration companies. Gold occurrences at Assean Lake (Kuiper et al., GS-18, this volume), located along strike from the exposed Archean craton margin at Gull Rapids, have been known since the 1930s. In addition, the map area is located at the Superior craton margin along strike from the economic Thompson Nickel and Fox River belts (Ni, Cu, PGE), and is host to Proterozoic mafic and ultramafic dikes (PGE). The completion of the structural study at Gull Rapids will provide a detailed geological framework to help guide future exploration programs along this portion of the Superior craton margin.

### Acknowledgments

This project is supported by an NSERC grant to S. Lin and by the Manitoba Geological Survey and Manitoba Hydro. The authors are largely indebted to Manitoba Hydro for logistical and financial support of the program in 2003 and 2004. Field assistance in 2004 by Tashia Dzikowski, Todd Middleton, Geoff Speers and Jennifer Vinck is greatly appreciated, as is the continued logistical support of Neill Brandson. Lawrence Norquay and Bill Reynolds (Manitoba Hydro), Custom Helicopters, Tataskweyak Cree Nation and Fox Lake First Nation are also thanked for their enthusiasm and support for the project throughout 2003 and 2004.



**Figure GS-15-18:** Outcrop photograph illustrating the forceful intrusion of a leucogranite dike into amphibolite, Gull Rapids map area. Injection seems to make space for itself by pushing apart the  $S_1$  foliation planes (which are planes of weakness).

## References

- Böhm, C.O., Bowerman, M.S. and Downey, M.W. 2003a: Bedrock mapping in the Gull Rapids area, northern Manitoba (NTS 54D6); *in* Report of Activities 2003, Manitoba Industry, Economic Development and Mines, Manitoba Geological Survey, p. 92–104.
- Böhm, C.O., Bowerman, M.S. and Downey, M.W. 2003b: Geology of the Gull Rapids area, Manitoba (NTS 54D6); Manitoba Industry, Economic Development and Mines, Manitoba Geological Survey, Preliminary Map PMAP2003-3, scale 1:5000.
- Heaman, L.M. and Corkery, M.T. 1996: U-Pb geochronology of the Split Lake Block, Manitoba: preliminary results; Trans-Hudson Orogen Transect, Report of Sixth Transect Meeting, Saskatoon, Saskatchewan, April 1–2, 1996, LITHOPROBE Secretariat, University of British Columbia, LITHOPROBE Report 55, p. 60–68.
- Lin, S. and Jiang, D., 2001: Using along-strike variation in strain and kinematics to define the movement direction of curved transpressional shear zones: an example from northwestern Superior Province, Manitoba; *Geology*, v. 29, p. 767–770.